# Probing the electronic transmission across a buried metal/metal interface

P. Moras,[1] D. Wortmann,[2] G. Bihlmayer,[2] L. Ferrari,[3] G. Alejandro,[4,5] P. H. Zhou,[4] D. Topwal,[4] P. M. Sheverdyaeva,[1] S. Blügel,[2] and C. Carbone[1]

[1]*Istituto di Struttura Materia, Consiglio Nazionale delle Ricerche, Trieste, Italy*

[2]*Institut für Festkörperforschung and Institute for Advanced Simulation, Forschungszentrum Jülich, D-52425 Jülich, Germany*

[3]*Istituto dei Sistemi Complessi, Consiglio Nazionale delle Ricerche, Roma, Italy*

[4]*International Center for Theoretical Physics (ICTP), I-34014 Trieste, Italy*

[5]*Centro Atómico Bariloche (CNEA), CONICET, 8400 San Carlos de Bariloche, Río Negro, Argentina*

(Received 1 July 2010; published 18 October 2010)

We monitored the *sp*-quantum-well states of Ag films on Pt(111) by angle-resolved photoemission in order to examine the electron transmission across the Ag/Pt interface. For thin layers up to 3.5 nm, the Ag states are characterized by broad quasiparticle peaks and a reversal of the parabolic curvature near the center of the surface Brillouin zone. Remarkable departures from the expected nearly-free-electronlike band dispersion persist in films of more than 14 nm thickness. First-principles calculations and symmetry analysis demonstrate that the observed anomalies in the spectroscopic data can be straightforwardly linked to variations in the Ag/Pt transmission coefficient in the energy-momentum space.

DOI: 10.1103/PhysRevB.82.155427 PACS number(s): 73.21.Fg, 79.60.Dp

## I. INTRODUCTION

Interfaces between bulk crystalline metals are one of the most basic building blocks of solid-state devices. Despite their fundamental importance, their experimental characterization is notoriously difficult. Many techniques probing the surface or bulk morphology of metals are available but often either they cannot reach a buried interface or lack the sensitivity to resolve the interface features. Even harder than the structural analysis is the determination of the electronic properties of interfaces. The degree of hybridization among Bloch states across an all-metal junction or, in other words, the transmission and reflection coefficients of a metal/metal interface, is essential to describe in detail the electrical current flow but it is difficult to determine experimentally. Transport measurements can give only quantities integrated in reciprocal space, including contributions from many different states in the vicinity of the Fermi level ($E_F$) of the system. On the other hand, the probing depth of energy- and momentum-resolved spectroscopic techniques is extremely limited due to the strong interaction of the electrons with matter (the inelastic mean-free path of electrons in solids is smaller than 2 nm for electron energies 10–1000 eV). Ideally, one should find a method to investigate the transmission coefficient of buried metal/metal interfaces at individual wave-vector values and different energies.

These requirements can be experimentally fulfilled by using the energy levels of a thin metal film as a means of investigation.[1] The junction between two semi-infinite crystals is replaced by an epitaxial metal layer grown on the surface of a metallic crystal. Due to quantum confinement effects and under suitable boundary conditions, the film valence electrons may give rise to discrete quantum-well (QW) states,[2–4] in analogy to the particle-in-a-box picture. These states can be regarded as two-dimensional waves, which bounce repeatedly between the surface and interface planes. By tuning their thickness-dependent band dispersion, they are forced to intercept at different locations of the energy-momentum space the surface-projected bands of the substrate and interact with them. If energy, momentum, and symmetry matching relations across the interface plane are satisfied, the film states (resonances) delocalize over the entire system. Truly confined QW states, instead, form in absence of such conditions. The degree of hybridization of the film states can be finally evaluated from their band dispersion and peak width by means of angle-resolved photoemission.

The success of the experiments described above depends critically on the materials. Silver is a good candidate for the formation of thin films. Epitaxial Ag layers with atomically uniform thickness can be grown on several (even lattice-mismatched) crystals. In addition, the *sp* bands of Ag are nearly-free-electronlike in the bulk and exhibit a parabolic in-plane dispersion in free-standing or weakly interacting films. Deviations from this simple functional form, expected in the case of strong coupling to the substrate, are easy to identify. For these reasons, several photoemission investigations have recently dealt with confinement effects in Ag. In a system where film and substrate have similar electronic and structural properties, such as for Ag on Au(111),[5,6] the QW state behavior agrees well with the predictions of simple models. In other cases, where junctions between dissimilar materials are formed, such as for Ag/W(110),[7] Ag/Au/W(110),[8] Ag/W(100),[9] and Ag/V(100),[10,11] the photoemission analysis reveals atypical band dispersion and peak-width variations in correspondence with the surface-projected bulk band edges of the substrate.

Here we report on an angle-resolved photoemission study of the *sp*-QW states which form in Ag(111) films grown on Pt(111).[12,13] Ag and Pt are face-centered-cubic (fcc) metals with moderate lattice mismatch [$a_{Ag}$=4.09 Å, $a_{Pt}$ =3.92 Å, $(a_{Ag}-a_{Pt})/(a_{Pt})\sim 4\%$] and similar bulk electronic structure, besides width and energy position of the *d* bands. In spite of these common features, the QW levels exhibit negative effective masses near the center of the surface Brillouin zone for the thinnest Ag layers and retain significant departures from the nearly-free-electronlike behavior in films

 

of more than 14 nm thickness. Symmetry analysis and first-principles calculations, performed for in-plane commensurate Ag/Pt systems, shed light onto the origin of the experimental observations. The anomalous band dispersion and spatial localization of the QW states are found to reflect the complex hybridization relations occurring between Ag and Pt bands with common symmetry and different in-plane dispersion. These findings demonstrate that spectroscopic investigations of thin metal films offer a viable way to map the energy- and momentum-dependent transmission coefficient of a buried metal/metal interface.

## II. EXPERIMENTAL AND COMPUTATIONAL DETAILS

The experiments were carried out at the VUV-Photoemission beamline on the Elettra synchrotron radiation facility in Trieste. The Pt(111) crystal was prepared by cycles of Ar-ion sputtering and annealing, alternated with oxygen exposures to remove surface contaminants. The clean Pt surface displayed a sharp hexagonal low-energy electron diffraction (LEED) pattern with a very low background. Ag films were grown on the substrate kept at 140 K and successively annealed to room temperature, to favor the formation of layers with atomically uniform thickness. The in-plane lattice parameters of Ag films thicker than 6 monolayers (MLs) (1 ML=2.36 Å), evaluated by comparing film and substrate LEED patterns, coincide with those of a Ag(111) crystal, although the diffraction spots appear to be more blurred. The photoemission measurement were performed along the $\bar{\Gamma}$-$\bar{M}$ surface direction at room temperature with 48 eV photons by mean of an R-4000 Scienta electron analyzer, which allows parallel acquisition of angle-resolved spectra over 30° angular range.

Our theoretical results were obtained by scalar relativistic *ab initio* density-functional theory (DFT) calculations within the local-density approximation[14] using the Jülich FLEUR code.[15] This code implements the full-potential linearized augmented plane-wave method[16] and the Green's-function embedding method[17] and thereby allows not only the effective treatment of transition-metal surfaces and interfaces but also the calculation of transport properties and truly semi-infinite surfaces. We applied this method to calculate the projected band structures of Ag(111) and Pt(111), the electronic transmission at the Ag(111)/Pt(111) interface and the Bloch spectral function for thin Ag films on Pt(111). In all our calculations, we used an fcc(111) unit cell with an averaged nearest-neighbor distance of 2.82 Å to enable the construction of a lattice-matched interface. This accounts for a 2% expansion (compression) of the lattice with respect to the experimental bulk Pt (Ag) lattice constants. The differences in the lattice constants were considered in a respective compression or expansion of the interlayer spacing.

## III. QUANTUM-WELL STATES AND INTERFACE TRANSMISSION

Figure 1(a) shows an intensity plot of the photoemission signal measured as a function of the momentum parallel to the surface $k$ along the $\bar{\Gamma}$-$\bar{M}$ axis for a 14 ML Ag film. The most prominent feature close to $E_F$ (saturated in the figure) is the Ag(111) Shockley surface state. The other structures, labeled with the quantum number $n$, are $sp$-derived QW states, arising from the finite film thickness. In a free-standing

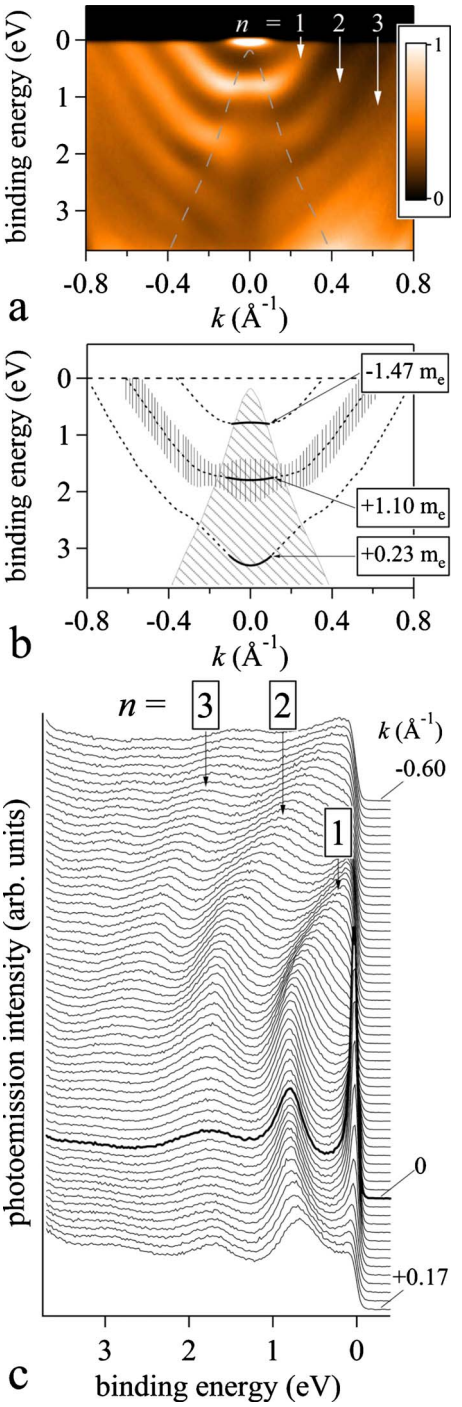


FIG. 1. (Color online) (a) Photoemission intensity map for a 14 ML Ag film on Pt(111). The dashed line encloses a region of diffuse photoemission intensity near $\bar{\Gamma}$. (b) Schematic band dispersion of the QW states displayed in (a). The effective masses of the bands are reported on the right-hand side. The vertical bars along the $n=2$ state indicate the full width at half maximum of the respective photoemission peaks. (c) Photoemission spectra as a function of $k$ corresponding to (a).

Ag(111) film, these states would show a nearly-free-electronlike parabolic dependence for $|k|<0.50$ Å$^{-1}$,[18] with energies of the band bottoms determined by the film thickness. The dispersion of the Ag QW states on Pt(111), instead, is nearly parabolic only at relatively large $k$ values. The reduced energy dispersion close to the center of the surface Brillouin zone results in an almost flat bottom for the $n=1, 2$ bands. The $n=3$ QW band displays changes in slope in the region about $k=\pm 0.4$ Å$^{-1}$ and a deep energy minimum at the $\bar{\Gamma}$ point. This behavior is described more quantitatively in Fig. 1(b), which reports the energy-momentum dependence of the QW peaks of Fig. 1(a). While moving toward $E_F$, the effective mass of the QW subbands $m_n$, derived from a parabolic fit to the data within the range $|k|<0.10$ Å$^{-1}$ and expressed in terms of the electron rest mass $m_e$, increases from $m_3=0.23m_e$ to $m_2=1.10m_e$ and, finally, changes sign for the $n=1$ state $(-1.47m_e)$.[10] For Ag(111) film structures, one would expect a totally different trend. First-principles calculations for a free-standing 13 ML Ag film give effective masses of $0.30m_e$, $0.27m_e$, and $0.20m_e$ for the $n=1,2,3$ QW states, respectively.[18] Experimentally, the QW effective masses for Ag layers grown on Ge(111),[19] Si(100),[20] Si(111),[20] and Cu(111) (Ref. 21) are always positive and vary between $0.2m_e-0.8m_e$ as a function of binding energy and film thickness.

Figure 1(c) reports a set of angle-resolved photoemission spectra corresponding to Fig. 1(a) within the range $-0.60<k<0.17$ Å$^{-1}$. In a Ag film with negligible substrate interactions, the intensity of the QW peaks is expected to fade monotonically as a function of $k$, due to the finite lateral coherence length of the potential well. The *sp*-Ag states located within the symmetry gap of Cu in Ag/Cu(111) systems, for instance, behave in accord with this model (Ref. 13). Figure 1(c) displays a much more complex situation for the Ag/Pt system. The $n=1$ peak, which is well defined in near normal emission geometry, remains sharp in the region of small dispersion and broadens only for $k$ vectors, where a significant increase in its energy dispersion can be seen. The width of the $n=2$ peak, on the other hand, shrinks while moving away from $\bar{\Gamma}$ and broadens slightly for $|k|>0.35$ Å$^{-1}$. This nonmonotonic $k$ dependence is displayed qualitatively in Fig. 1(b) by mean of the vertical bars, which represent the full at half maximum of the photoemission peaks for the $n=2$ band. Finally, the $n=3$ state, which is hard to identify near $k=0$, exhibits a behavior qualitatively similar to that of the $n=2$ state. Notably, a diffuse photoemission signal characterizes the region where the QW states deviate more strongly from the simple parabolic behavior and the width of the quasiparticle peaks are broad. The dashed line in Fig. 1(a) and the dashed area in Fig. 1(b) identify this zone.

Details of energy dispersion and thickness dependence of the *sp*-derived states are well discernible in the photoemission intensity maps presented in Fig. 2. The panels refer to Ag films of (a) 22, (b) 45, and (c) 60 ML thickness. All QW bands display deviations from the simple parabolic behavior in the region enclosed by the dashed lines, already shown in Fig. 1(a). These effects become gradually weaker with increasing the film thickness. However, they do not vanish

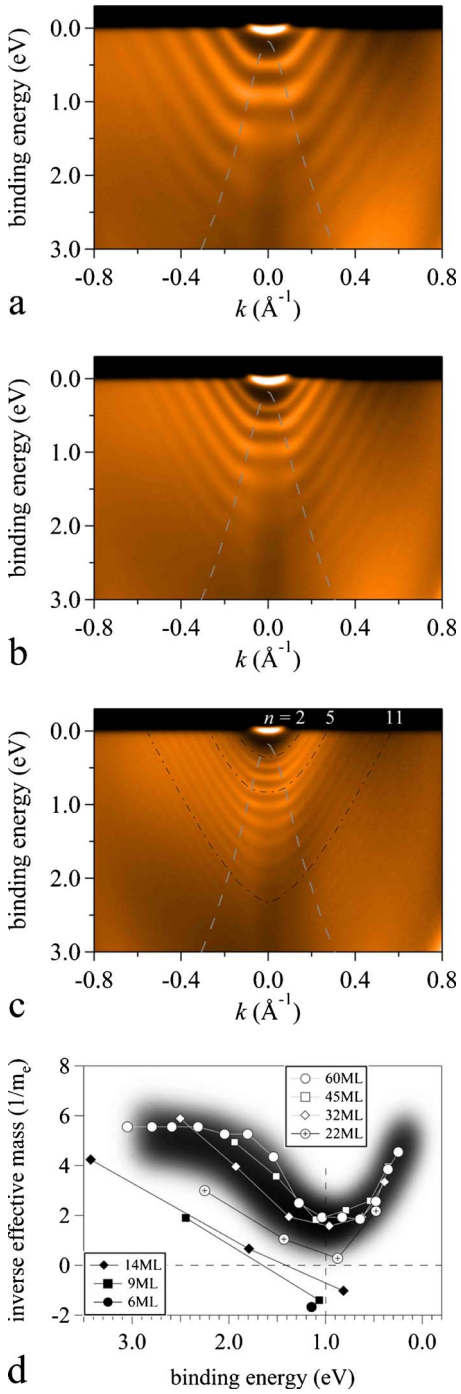


FIG. 2. (Color online) Photoemission intensity maps for (a) 22, (b) 45, and (c) 60 ML Ag films on Pt(111). All panels report the dashed line displayed in Fig. 1(a). (d) Inverse effective masses for several film thicknesses. The gray, blurred curve highlights the binding energy dependence of the effective masses for thick (≥22 ML) films.

completely and are still detectable in films as thick as 60 ML. In Fig. 2(c), dotted-dashed lines are used to highlight the band dispersion of the $n=2,5,11$ QW states. The band bottom appears to be flatter for the $n=5$ state than for other states lying at higher and lower binding energy. Similar trends are detectable also for thinner layers [Figs. 2(a) and

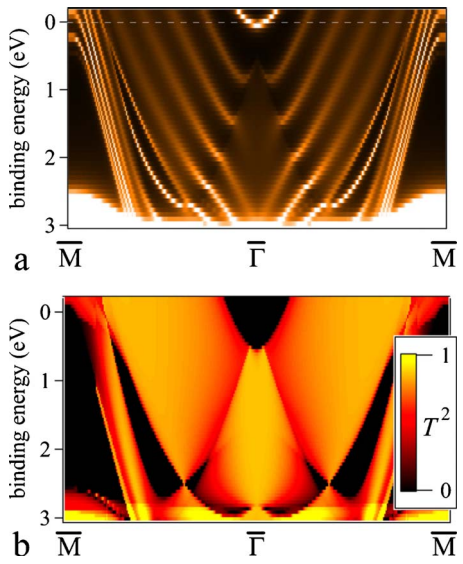


FIG. 3. (Color online) (a) Calculated Bloch spectral function for a 10 ML Ag film on semi-infinite Pt(111). The $\bar{\Gamma}$-$\bar{\mathrm{M}}$ distance corresponds to 1.28 $\text{Å}^{-1}$. The onset of the *d* bands below 3 eV is clearly visible. (b) Calculated energy-momentum map of the transmission probability ($T^2$) for the Ag/Pt(111) interface. Lighter colors identify regions of higher transmission.

2(b)], whose energy levels near the $\bar{\Gamma}$ point appear to be extremely flat at about 1 eV below $E_F$.

In order to summarize the results of the photoemission data, Fig. 2(d) reports the inverse effective mass for the QW bands of several Ag films as a function of the binding energy. For the thinnest layers (full symbols), the inverse effective mass displays a linear dependence on the binding energy, with negative values near 1.0 eV. With increasing the film thickness, all values become positive (open symbols) but a minimum is clearly detectable for each film thickness at about 1.0 eV. Notably, the functional dependence of the inverse masses, highlighted by a blurry gray curve in the figure, persists in films of considerably high thickness, without approaching the constant behavior that would be expected asymptotically. Due to the electron escape depth, which is shorter than 6 Å in the present experimental conditions, the photoemission measurements directly probe only states with significant charge density in the topmost Ag film layers. Nevertheless, the effects of coupling to the substrate modify the band dispersion relations of the QW states which, being spatially extended, propagate over the whole film thickness. This can be regarded as a result of the boundary conditions imposed by the substrate, with effects obviously not merely localized at the interface.

The experimental findings can be understood by DFT calculations, examining the electronic structure of bulk Pt and Ag crystals, thin Ag films, and the Ag/Pt interface. Figure 3(a) shows the Bloch spectral function for a 10 ML Ag film on a semi-infinite Pt(111) substrate, calculated along the $\bar{\Gamma}$-$\bar{\mathrm{M}}$ axis. To mimic the photoemission experiment, the contributions from all Ag planes were added with an exponentially decaying weight factor corresponding to a photoelectron escape depth of approximately 4 ML. In the analysis of angle-resolved photoemission data, the Bloch spectral function has the same significance of the density of states for angle-integrated measurements. In our case, we try to use the Bloch spectral function to interpret the experimental results while keeping in mind that: (i) final state or matrix-element effects are not included in the calculations; (ii) our treatment does not incorporate any *k*-dependent lifetime reduction in the QW states; (iii) the intrinsic lifetime of the single-particle states is simply approximated by a small imaginary energy of 27 meV for all states. Despite these restrictions, our theoretical picture catches in detail all features characterizing the electronic structure of the Ag/Pt system. We identify a triangular area of diffuse background intensity, where substantial differences from the nearly-free-electronlike behavior are observed. Within this region, the $n=1$ state, hardy discernible near $\bar{\Gamma}$ due to its low spectral weight, exhibits a negative effective mass. The $n=2$ state tends to vanish while approaching the $\bar{\Gamma}$ point and has a positive effective mass. The $n=3$ state, finally, shows a deep energy minimum. Notably, the dispersions of all QW bands seem to exhibit a kink at the edges of the triangular area, in correspondence with a narrowing of the quasiparticle peaks. Outside the triangular region all states tend to broaden gradually, but moderately, as a function of *k*, with effects more evident for larger *k* values. Our theoretical results demonstrate that the observed peak broadening in the Ag/Pt system is largely attributable to hybridization effects, and only to a lesser extent to the loss of coherence in the potential well.

To understand these features in detail, we have to consider the relevant electronic structure of the bulk materials in terms of the surface-projected band structure. As shown in Fig. 4(a), a single band (dark brown/gray area) is present in Ag at binding energies up to 3 eV below $E_F$. This upward dispersing *sp* band is symmetric along the $\bar{\Gamma}$-$\bar{\mathrm{M}}$ direction with respect to the remaining mirror plane. In a thin Ag film, the continuum of states in the projected band structure becomes discrete and depending on the interaction with the Pt substrate fully localized QW states or resonances are formed. As the hybridization is only possible with states of the same symmetry, we have to consider the projected band structure of symmetric states in Pt [Fig. 4(b)]. Here areas with zero (black), one (dark brown/gray), two (light brown/gray), and three (white) Bloch states can be identified. At the $\bar{\Gamma}$ point, the band diagram is defined by the projection of the Pt states along the Γ-L bulk line [Fig. 4(c)]. While moving from L to Γ, we find a doubly degenerate $\Lambda_3$ band which disperses downwards from $E_F$ to 1.5 eV binding energy. About 0.2 eV below $E_F$, the (symmetric) $\Lambda_1$ band disperses also downward, leading to two states in this region [light brown/gray segment at $\bar{\Gamma}$ in Fig. 4(b)]. Around 1.5 eV, the $\Lambda_3$ band exhibits a flat minimum before it reaches Γ at 1.5 eV. Therefore, we observe three states in the region between 1.5 and 1.6 eV binding energy [white segment at $\bar{\Gamma}$ of Fig. 4(b)].

Leaving the Γ-L line in Fig. 4(c), we find antisymmetric bands labeled with (2) that do not contribute to the band diagram of Fig. 4(b). More significantly we identify sharply upward dispersing states originating from the $\Lambda_3$ band, like the symmetric (1) band along the L-X bulk line. Along the

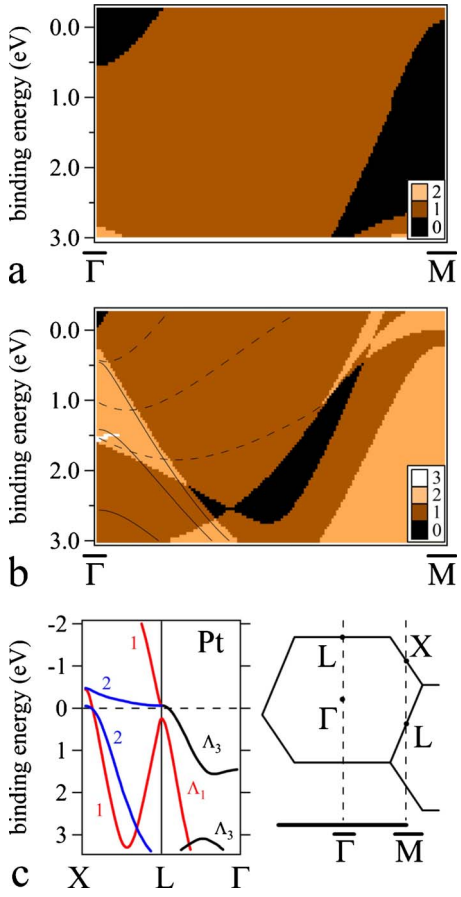


FIG. 4. (Color online) Bulk band structure of (a) Ag and (b) Pt projected on the $\bar{\Gamma}$-$\bar{M}$ surface axis (only states symmetric with respect to the mirror plane are shown). The projection is schematically displayed in (c), together with the Pt bands, labeled according to symmetry, along the X-L-Γ bulk line. The continuous and dashed lines in panel (b) display the energy-momentum dependence of the bands originating from states with $\Lambda_1$ and $\Lambda_3$ symmetry at $\bar{\Gamma}$, respectively.

$\bar{\Gamma}$-$\bar{M}$ direction bands of this type give rise to states which disperse downward in the vicinity of $\bar{\Gamma}$ and upward at larger $k$ values. Their energy-momentum relations are exemplified in Fig. 4(b) for some $k_z$ values by thin dashed lines. Another (1) band can be seen to disperse sharply downwards from the $\Lambda_1$ band along L-X. When bands of this kind are projected along the $\bar{\Gamma}$-$\bar{M}$ direction the resulting states lay within a triangular region close to $\bar{\Gamma}$, corresponding well to the area where the experimental results identified departures from the nearly-free-electronlike model. The band dispersion of the Pt states in this region is sketched in Fig. 4(b) by thin continuous lines. From this picture it is evident that the Ag states near $k=0$ pick up the character of the corresponding Pt states. The negative effective mass for thin Ag layers, the atypical minimum in the inverse effective mass for thick Ag layers, as well as the low spectral weight of the QW states near $\bar{\Gamma}$, reflect the high degree of hybridization between the Ag and Pt states within the triangular area.

The most interesting aspect of our study is the ability to infer the properties of the Ag/Pt transmission coefficient $T$ from the analysis of the spectroscopic data for Ag films on Pt(111). Truly localized QW states form only if the film boundaries are perfectly reflecting ($T=0$). On the other hand, if the interface showed perfect transmission ($T=1$), the electronic states of the Ag layer would be indistinguishable from those of the Pt substrate in a photoemission experiment. Any finite transmission between these two limits ($T=0$ or 1) leads to the formation of resonances in the Ag film, whose linewidth and intensity give a measure of the degree of transmission at the interface. Figure 3(b) shows the transmission probability $T^2$ of the Ag/Pt(111) interface, calculated for the $k$ points along the $\bar{\Gamma}$-$\bar{M}$ direction. Transmission can occur only for energies and $k$ values at which there are states in both Ag and Pt. Hence the gaps in the projected band structures of the two materials, shown in black in Figs. 4(a) and 4(b), result in the areas of zero transmission in Fig. 3(b). High transmission characterizes most of the area occupied by the Ag states, especially close to $\bar{\Gamma}$ and halfway from $\bar{\Gamma}$ to the zone boundary. A notable exception is the reduced transmission along the band edge marked by the dashed line of Fig. 1, in correspondence with the recovery of the parabolic band dispersion and sharpening of the QW peaks. From Fig. 3(b) it is evident that the observed $k$ dependence of the QW peak width, associated with changes in the degree of hybridization between Ag and Pt states, catches in detail the fine structure of the transmission probability in the energy-momentum space.

## IV. SURFACE STATE

For the thinnest layers, the interaction between Ag and Pt states affects not only the QW states but also the Ag(111) surface state. In analogy to other systems, such as Ag films on Ge(111),[22] when the film thickness is reduced to few atomic layers the surface-state wave function is sufficiently delocalized into the film to feel presence of the supporting material. For the Ag/Pt system, the effects of coupling become clearly distinguishable for a 6 ML Ag film. Figure 5 reports photoemission data for this film thickness. The photoemission intensity map in the panel on the top-right of the figure displays the surface state as a bright feature, whose parabolic dispersion is highlighted with a continuous black line. In contrast with the observations for thicker Ag films (Figs. 1 and 2), the surface-state peak appears to be much broader, with a tail that extends to a binding energy of about 0.45 eV. Interestingly, the intensity of this tail drops more steeply as a function of the binding energy near $\bar{\Gamma}$ than at larger $k$. This behavior can be visualized in the momentum distribution curves of Fig. 5. These lines represent cuts of the photoemission map at constant energies, taken every 15 meV from 0.6 eV binding energy (bottommost line). The thicker lines display the intensity of the photoemission signal at the band bottom of the surface state (75 meV) and at an energy where the $k$-dependent intensity drop gives rise to a dip around $k=0$ (240 meV).

A very similar picture can be obtained in our *ab initio* calculations for a 4 ML Ag film on semi-infinite Pt(111),

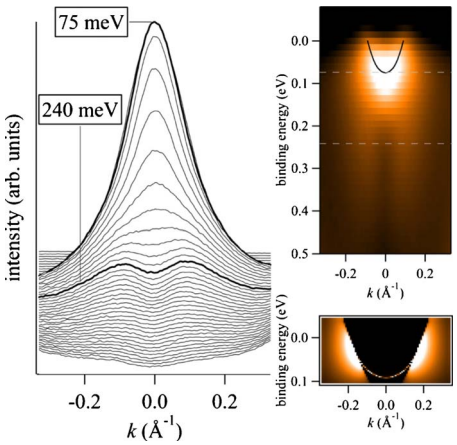


FIG. 5. (Color online) Experimental momentum distribution curves for the Ag(111) Shockley surface state derived from the intensity map displayed in the top-right panel (Ag film thickness 6 ML). The bottom-right panel shows the result of first-principles calculations for a 4 ML Ag film on semi-infinite Pt(111).

which are reported in the panel on the bottom-right corner of the figure. Very close to $\bar{\Gamma}$, the surface state shows no broadening. Actually, the width of the surface-state intensity in the Bloch spectral function of the surface layer is purely due to a small imaginary part of the energy, introduced for technical reasons of visualization. That is, this state is a surface state with infinite lifetime in our calculation, as it is expected from the projected band structures of Ag and Pt, both having gaps at the surface-state energy at $\bar{\Gamma}$. This situation changes as soon as one considers the behavior of the surface state at larger $k$ values. Along its energy dispersion, the surface state intercepts a continuum of surface-projected Pt bands with which hybridization is allowed. As a consequence, the surface states turns into a resonance with a finite lifetime. This change in the degree of hybridization manifests in a photoemission experiment as a $k$-dependent broadening of the quasiparticle peaks.

## V. CONCLUSIONS

In this paper, we demonstrate that the *sp*-QW states of Ag films on Pt(111) can be employed as a probe of the hybridization strength between the two metals. By combining the results of photoemission experiments and theoretical analysis, we are able to establish a detailed correspondence between band dispersion and quasiparticle peak width of the Ag QW states and the electronic transmission across the Ag/Pt interface. This method can be applied to map the transmission coefficient of junctions between thin metal films and bulk metal substrates that mimic realistically semi-infinite all-metal junctions.

[1] M. K. Brinkley, Y. Liu, N. J. Speer, T. Miller, and T.-C. Chiang, Phys. Rev. Lett. **103**, 246801 (2009).
[2] T.-C. Chiang, Surf. Sci. Rep. **39**, 181 (2000).
[3] M. Milun, P. Pervan, and D. P. Woodruff, Rep. Prog. Phys. **65**, 99 (2002).
[4] P. Pervan and M. Milun, Surf. Sci. **603**, 1378 (2009).
[5] T. Miller, A. Samsavar, G. E. Franklin, and T.-C. Chiang, Phys. Rev. Lett. **61**, 1404 (1988).
[6] L. Huang, X. G. Gong, E. Gergert, F. Forster, A. Bendounan, F. Reinert, and Z. Zhang, EPL **78**, 57003 (2007).
[7] D. V. Vyalikh, Yu. Kucherenko, F. Schiller, M. Holder, A. Kade, S. L. Molodtsov, and C. Laubschat, Phys. Rev. B **76**, 153406 (2007); A. M. Shikin, D. V. Vyalikh, G. V. Prudnikova, and V. K. Adamchuk, Surf. Sci. **487**, 135 (2001).
[8] A. M. Shikin, D. V. Vyalikh, Yu. S. Dedkov, G. V. Prudnikova, V. K. Adamchuk, E. Weschke, and G. Kaindl, Phys. Rev. B **62**, R2303 (2000).
[9] A. M. Shikin, M. B. Visman, G. G. Vladimirov, V. K. Adamchuk, and O. Rader, Surf. Sci. **600**, 2681 (2006).
[10] T. Valla, P. Pervan, M. Milun, A. B. Hayden, and D. P. Woodruff, Phys. Rev. B **54**, 11786 (1996).
[11] M. Kralj, Surf. Sci. **599**, 150 (2005).
[12] Two-photon photoemission analysis of the image states of Ag films on Pt(111) can be found in S. Smadici, D. Mocuta, and R. M. Osgood, Phys. Rev. B **69**, 035415 (2004); S. Smadici and R. M. Osgood, *ibid.* **71**, 165424 (2005).
[13] The *d* levels of the related system Ag/Pd(111) have been thoroughly investigated by angle-resolved photoemission in I. Pletikosić, V. Mikšić Trontl, M. Milun, D. Šokčević, R. Brako, and P. Pervan, J. Phys.: Condens. Matter **20**, 355004 (2008); V. Mikšić Trontl, I. Pletikosić, M. Milun, P. Pervan, P. Lazić, D. Šokčević, and R. Brako, Phys. Rev. B **72**, 235418 (2005).
[14] S. H. Vosko, L. Wilk, and M. Nusair, Can. J. Phys. **58**, 1200 (1980).
[15] For a program description, see http://www.flapw.de
[16] E. Wimmer, H. Krakauer, M. Weinert, and A. J. Freeman, Phys. Rev. B **24**, 864 (1981).
[17] D. Wortmann, H. Ishida, and S. Blügel, Phys. Rev. B **66**, 075113 (2002).
[18] P. Moras, D. Topwal, P. M. Sheverdyaeva, L. Ferrari, J. Fujii, G. Bihlmayer, S. Blügel, and C. Carbone, Phys. Rev. B **80**, 205418 (2009).
[19] S.-J. Tang, W.-K. Chang, Y.-M. Chiu, H.-Y. Chen, C.-M. Cheng, K.-D. Tsuei, T. Miller, and T.-C. Chiang, Phys. Rev. B **78**, 245407 (2008).
[20] I. Matsuda, T. Ohta, and H. W. Yeom, Phys. Rev. B **65**, 085327 (2002).
[21] M. A. Mueller, T. Miller, and T.-C. Chiang, Phys. Rev. B **41**, 5214 (1990).
[22] S.-J. Tang, T. Miller, and T.-C. Chiang, Phys. Rev. Lett. **96**, 036802 (2006).